Metabolism Open 25 (2025) 100354

Contents lists available at ScienceDirect

Metabolism Open

journal homepage: www.sciencedirect.com/journal/metabolism-open

Lipidomics reveals potential biomarkers and pathophysiological insights in the progression of diabetic kidney disease

Xiaozhen Guo [a,b,1], Zixuan Zhang [a,b,1], Cuina Li [b,1], Xueling Li [a,1], Yutang Cao [c], Yangyang Wang [b,d], Jiaqi Li [b,e], Yibin Wang [b,e], Kanglong Wang [b], Yameng Liu [b], Cen Xie [b,c,e,*], Yifei Zhong [a,**]

[a] Department of Nephrology A, Longhua Hospital, Shanghai University of Traditional Chinese Medicine, Shanghai, PR China
[b] State Key Laboratory of Drug Research, Shanghai Institute of Materia Medica, Chinese Academy of Sciences, Shanghai, PR China
[c] School of Chinese Materia Medica, Nanjing University of Chinese Medicine, Nanjing, 210023, PR China
[d] School of Pharmaceutical Science and Technology, Hangzhou Institute for Advanced Study, University of Chinese Academy of Sciences, Hangzhou, 310024, PR China
[e] University of Chinese Academy of Sciences, Beijing, 100049, PR China

ARTICLE INFO

Keywords:
Diabetes kidney disease
Diabetes mellitus
Lipidomics
Biomarker
Lysophosphatidylethanolamines

ABSTRACT

Background: Diabetic kidney disease (DKD) is the leading cause of end-stage renal disease, affecting over 30 % of diabetes mellitus (DM) patients. Early detection of DKD in DM patients can enable timely preventive therapies, and potentially delay disease progression. Since the kidney relies on fatty acid oxidation for energy, dysregulated lipid metabolism has been implicated in proximal tubular cell damage and DKD pathogenesis. This study aimed to identify lipid alterations during DKD development and potential biomarkers differentiating DKD from DM.
Methods: lipidomics analysis was performed on serum collected from 55 patients with DM, 21 with early DKD stage and 32 with advanced DKD, and 22 healthy subjects. Associations between lipids and DKD risk were evaluated by logistic regression.
Results: Lipid profiling revealed elevated levels of certain lysophosphatidylethanolamines (LPEs), phosphatidylethanolamines (PEs), ceramides (Cers), and diacylglycerols (DAGs) in the DM-DKD transition, while most LPEs, lysophosphatidylcholines (LPCs), along with several monoacylglycerol (MAG) and triacylglycerols (TAGs), increased further from DKD-E to DKD-A. Logistic regression indicated positive associations between LPCs, LPEs, PEs, and DAGs with DKD risk, with most LPEs correlating significantly with urinary albumin-to-creatinine ratio (UACR) and inversely with estimated glomerular filtration rate (eGFR). A machine-learning-derived biomarker panel, Lipid9, consisting of LPC(18:2), LPC(20:5), LPE (16:0), LPE (18:0), LPE (18:1), LPE (24:0), PE (34:1), PE (34:2), and PE (36:2), accurately distinguished DKD (AUC: 0.78, 95 % CI 0.68–0.86) from DM. Incorporating two clinical indexes, serum creatinine and blood urea nitrogen, the Lipid9-SCB model further improved DKD detection (AUC: 0.83, 95 % CI 0.75–0.90) from DM, and was notably more sensitive for identifying DKD-E (AUC: 0.79, 95 % CI 0.67–0.91).

Abbreviations: Aclycar, Aclycarnitine; ALT, Alanine aminotransferase; AST, Aspartate transaminase; AMPK, AMP-activated protein kinase; AUC, Area under ROC curve; BUN, Blood urea nitrogen; Cer, Ceramide; CE, Cholesterol ester; CI, Confidence interval; CKD-EPI, Chronic Kidney Disease Epidemiology Collaboration; Ctrl, Control; CVD, Cardiovascular disease; DM, Diabetes mellitus; DAG, Diacylglycerol; DKD, Diabetic kidney disease; DKD-A, Advanced stage of DKD; DKD-E, Early stage of DKD; eGFR, Estimated glomerular filtration rate; ESRD, End-stage renal disease; FFA, Free fatty acid; HbA1c, Glycosylated hemoglobin, type A1c; HDL-C, High-density lipoprotein cholesterol; LacCer, Lactosylceramide; LASSO, Least absolute shrinkage and selection operator; LDL-C, Low-density lipoprotein cholesterol; LPA, Lysophosphatidic acid; LPC, Lysophosphatidylcholine; LPE, Lysophosphatidylethanolamine; MAG, Monoacylglycerol; OR, Odds ratio; PA, Phosphatidic acid; PC, Phosphatidylcholine; PE, Phosphatidylethanolamine; PKC, Protein kinase C; PLA2, Phospholipase A2; PLS-DA, Partial least squares-discriminant analysis; PP2A, Protein phosphatase 2A; PS, Phosphatidylserine; PI, Phosphatidylinositol; PG, Phosphatidylglycerol; Q-TOF mass spectrometer, Quadrupole time-of-flight mass spectrometer; RF, Random forest; ROC, Receiver operating characteristic curve; SCr, Serum creatinine; SM, Sphingomyelin; SVM-RFE, Support vector machine-recursive feature elimination; TAG, Triacylglycerol; TC, Total cholesterol; UACR, Urinary albumin-to-creatinine ratio; UHPLC, Ultra performance liquid chromatography.

* Corresponding author. State Key Laboratory of Drug Research, Shanghai Institute of Materia Medica, Chinese Academy of Sciences, Shanghai, PR China.
** Corresponding author.
E-mail addresses: xiecen@simm.ac.cn (C. Xie), yifeilily@126.com (Y. Zhong).
[1] These authors contributed equally to this work.

https://doi.org/10.1016/j.metop.2025.100354
Received 14 January 2025; Received in revised form 27 February 2025; Accepted 1 March 2025
Available online 3 March 2025
2589-9368/© 2025 The Authors. Published by Elsevier Inc. This is an open access article under the CC BY-NC-ND license (http://creativecommons.org/licenses/by-nc-nd/4.0/).

Conclusion: This study deciphers the lipid signature in DKD progression, and suggests the Lipid9-SCB panel as a promising tool for early DKD detection in DM patients.

1. Introduction

Diabetes mellitus (DM) is a metabolic disease characterized by hyperglycemia that is spreading globally [1], with approximately 10.5 % of adults aged 20–79 years suffering from DM, which is expected to increase to 12.2 % by 2045 [2]. This surge poses a profound threat to public health. Among the myriad complications associated with DM, diabetic kidney disease (DKD) emerges as the most prevalent microvascular complication, impacting over 30 % of individuals afflicted with DM [3]. DKD has become the leading cause of end-stage renal disease (ESRD), significantly heightening the risk of cardiovascular disease (CVD) mortality of CVD mortality [4,5]. Early detection of DKD may enable early initiation of appropriate preventive therapy that can delay or even halt disease progression. However, the progression of DM to DKD, and ultimately to ESRD, is often considered inevitable, even in case where glycemic control is achieved. Despite advancements in managing blood glucose levels, the effectiveness of therapies aimed at mitigating the progression from DM to DKD and ESRD remains limited, primarily due to the challenges associated with the early detection of DKD.

DKD is characterized by dysfunction of the glomerular filtration barrier and a decline in renal function, manifesting as persistent elevation of urinary albumin and progressive reduction in estimated glomerular filtration rate (eGFR), respectively [6]. In clinical practice, microalbuminuria and eGFR serve as pivotal indicators for the early detection and monitoring of DKD progression. However, the trend of renal impairment in DKD patients does not always align with the increase in proteinuria, particularly in early-stage DKD [7]. Notably, the prevalence of DKD patients with an eGFR <60 mL/min/1.73 m^2 but without proteinuria has steadily increased over the past 30 years [8]. Alarmingly, during this period, the annual mortality rate of these patients increased from 3.5 % to 5.1 % [9]. In addition, studies have shown that some DKD patients, with or without intervention, revert to baseline microalbuminuria levels, without developing macroalbuminuria [10,11]. A meta-analysis further suggested that nearly half of DKD diagnoses by physicians are inaccurate when based solely on basic clinical information such as proteinuria and eGFR. Hence, there is an urgent need to identify more precise diagnostic biomarkers that can effectively discern the progression from DM to DKD, especially for the early stage of DKD.

Lipids are essential molecules vital for the sustenance of living organisms, with lipid metabolites functioning as signaling molecules that regulate various pathways [12]. Kidney epithelial cells have high energy demands, largely met through fatty acid oxidation [13]. In recent years, abnormal lipid metabolism has garnered increasing attention as pivotal contributor to proximal tubular cell damage and DKD pathology. Previous research suggests that impaired cholesterol metabolism, enhanced lipid uptake or synthesis, and dysregulated fatty acid oxidation, collectively contribute to lipid droplet accumulation, reactive oxygen species generation, mitochondrial damage, and the progression of DKD [14,15]. It has been reported that sphingomyelin (SM) and phosphatidylcholine (PC) tend to increase with the progression of DKD and are associated with renal impairment and all-cause mortality [16]. Furthermore, lysophosphatidylethanolamine (LPE), phosphatidylethanolamine (PE), and triacylglycerol (TAG) levels have been found to be significantly elevated in DKD serum samples and closely correlated with DKD staging [17]. A better understanding of these metabolic processes could unlock novel therapeutic strategies targeting lipid metabolism in kidney diseases. Despite the established associations between abnormal lipids with DKD, significant research gaps remain in elucidating the specific lipid remodeling patterns during the onset of DKD and identifying the lipid species involved in its progression across different stages.

To address this, we performed a mass spectrometry-based serum untargeted lipidomics from a cross-sectional cohort that included patients diagnosed with DM and early/advanced stage of DKD (DKD-E/A), as well as control individuals (Fig. 1). The serum lipidome analysis revealed distinct lipid profiles marking the onset of DKD compared to DM, characterized by elevated levels of LPEs, PEs, LPCs, ceramides (Cers), and diacylglycerols (DAGs). Additionally, LPEs, lysophosphatidylcholines (LPCs), monoacylglycerols (MAGs) and TAGs levels were further elevated from DKD-E to DKD-A. Among these lipids, most LPEs exhibited a strong positive correlation with urinary albumin-to-creatinine ratio (UACR) and an inverse correlation with eGFR, two key indicators of renal function. To identify potential lipid biomarkers, we employed machine learning algorithms and developed a panel termed Lipid9-SCB. This panel comprises nine lipid species primarily from the LPE, PE, LPC, and DAG classes, combined with two clinical indices of kidney function: serum creatinine (SCr) and blood urea nitrogen (BUN). The Lipid9-SCB panel effectively distinguished DKD from DM population and differentiating DKD stages, and its diagnostic accuracy surpassed that of eGFR in detecting DKD, particularly in DKD-E. Our findings of a distinct lipid fingerprint at the early stage of DKD, coupled with their associations with makers of disease severity, suggest that these lipids may play a role in kidney dysfunction during the early development of DKD. Therefore, the Lipid9-SCR panel holds promise as a valuable tool for the early detection of DKD.

2. Materials and methods

2.1. Participants' characteristics

In this study, serum samples from patients hospitalized at Longhua Hospital of Shanghai University of Traditional Chinese Medicine between September 2022 and May 2023 were collected for subsequent lipid metabolomics studies. After obtaining individual informed consent, 130 patients were enrolled in the study, including 55 patients with DM, 21 patients with DKD-E, 32 patients with DKD-A, and 22 control populations (Ctrl). The DKD-E was defined as diabetes with CKD stage A2, G1/2, namely UACR between 30 and 300 mg/g and eGFR >60 mL/min/1.73 m^2, whereas DKD-A was defined as diabetes with CKD stage A3 or G3/4/5, namely UACR >300 mg/g or eGFR <60 mL/min/1.73 m^2, respectively [18–20], where eGFR was calculated according to the Chronic Kidney Disease-Epidemiology Collaboration (CKD-EPI) equation [21,22]. The control group was derived from the inpatient medical examination population. All these individuals or their legal representatives as well as the ethics committees of the participating hospitals gave their consent for the histological study of the biobank materials. The study was approved by the Ethics Committee of Longhua Hospital, Shanghai University of Traditional Chinese Medicine (2021LCSY128). All participants signed a consent form allowing the use of their serum samples for lipidomics studies.

2.2. Lipidomics analysis

The serum lipidome was analyzed using a high-coverage lipidomic approach as described previously [14]. Lipids were extracted from serum using a methanol/water/chloroform mixture. The organic phases were evaporated to dryness under vacuum. Lipidomics analysis was performed using an I-Class UPLC coupled to a Q-TOF mass spectrometer (Waters Corp., Milford, MA, USA). Firstly, the organic extracts were first reconstituted in chloromethane: methanol (1:1, v/v) solution, and

secondly diluted with isopropanol: acetonitrile: water (2:1:1, v/v/v) solution. The samples were then subjected to gradient elution on a CSH column (Waters UPLC CSH 2.1 × 100 mm, i.d. 1.7 μm, Waters Corp.) under positive and negative ionization modes, respectively.

The Q-TOF mass spectrometer was operated with a mass resolution of 22,000 and a scanning range of *m/z* 50−1500. The untargeted lipidomics data were processed using the Progenesis QI software (version 3.0, Waters Corp., Milford, MA, USA), and the final output of the "feature" table was exported to SIMCA (Sartorius, version 16.0) software for multivariate analysis. LipidMaps, LipidBlast, METLIN, and HMDB databases were applied for lipid identification. Finally, R v4.0.4 and Rstudio v1.3.1056 softwares were utilized along with heatmap packages such as ggplot2, ggpubr, and complexHeatmap to present the data.

2.3. Statistical analysis

All data were presented as mean ± SEM. The Student's *t*-test was used for analysis of two groups, and one-way ANOVA followed by Tukey's post hoc correction was used for analysis of multiple groups. $p < 0.05$ was considered to be significant. Simple associations were tested by Pearson correlation analysis. PLS-DA was performed to examine the lipidomes differences between the Ctrl, DM, DKD-E and DKD-A groups using the R package ropls (1.36.0). We identified the most common profiles (clusters) during progression of DM to different stages of DKD

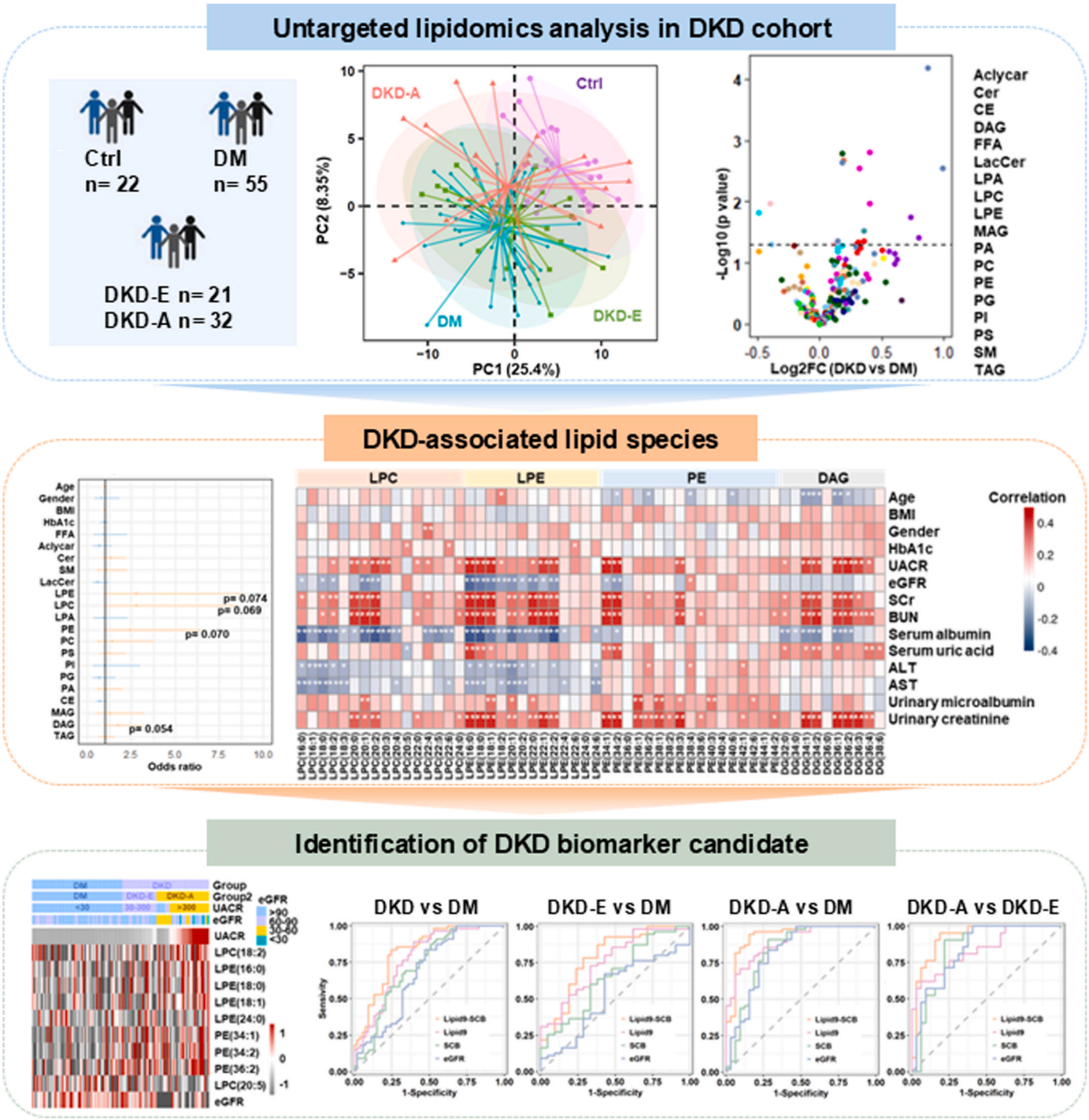

Fig. 1. A framework for identifying lipid alteration during DM progression to DKD and potential biomarker for the early detection of DKD.

using the R package mFuzz (2.64.0). Logistic regression was used to examine the association of each lipid class or lipid species with the risk of DKD versus DM; odds ratios and 95 % CIs were expressed for one SD change in each explanatory variable.

We applied multiple methods of machine learning [23], including least absolute shrinkage and selection operator (LASSO) regression method [24], support vector machine-recursive feature elimination (SVM-RFE) [25], and random forest (RF) [26], using the R packages glmnet (4.1.8), caret (6.0.94), and randomForest (4.7.1.2), respectively, to identify the most predictive biomarkers. For the LASSO analysis, we chose the optimal value of the debugging parameter λ to maximize the percentage of correctly identified diseases/controls and performed 10-fold cross-validation. RF is based on multiple decision trees, so it has the advantage of reducing the likelihood of overfitting, thus helping us to rank predict the most important variables. SVM uses a linear boundary called hyperplane to divide the data into groups of similar elements and is considered as a robust method. We perform feature selection based on SVM algorithm and calculate the correctness rate by 10-fold cross validation. Receiver operating characteristic curve (ROC) analysis evaluates the discriminative ability of the model. The overall diagnostic performance of the model was assessed by the area under ROC curve (AUC). Statistical analyses were run using R software (4.4.1).

3. Results

3.1. Characteristics of the study cohort

The study cohort comprised the following groups: the DM group (n = 55), the DKD-E group (n = 21), the DKD-A group (n = 32), and the Ctrl groups (n = 22). The cohort included 59 males and 71 females, aged 25–82 years, with body mass indices ranging from 17.0 to 43.2. Baseline clinical and laboratory data are summarized in Table 1. The levels of glycosylated hemoglobin, specifically type A1C (HbA1c), were markedly elevated in both the DM (7.5 %) and DKD (7.4 %) groups compared to the control group (5.6 %). However, there was no significant difference in HbA1c levels between the DM and DKD groups. SCr levels were highest in the DKD group, particularly in the DKD-A group, which is a major determinant of eGFR. The mean eGFR for DKD-A patients was 64.8 mL/min/1.73 m^2, significantly lower than that for DKD-E patients (93.9 mL/min/1.73 m^2). This suggests that kidney damage was more severe in DKD-A patients than that in the DKD-E group. In addition, UACR, another indicator of renal function decline, was significantly higher in both DKD-E (103.0 ± 70.2 mg/g) and DKD-A (937.8 ± 1048.0 mg/g) compared to the DM (9.6 ± 6.1 mg/g) and control (5.8 ± 2.9 mg/g) groups. BUN levels did not differ significantly among the control, DM, and DKD-E groups, but showed a significant increase in the DKD-A group compared to the control and DM groups as the disease progressed. Finally, in terms of blood lipid, TAG levels were significantly higher in DKD-A patients compared to DM patients, while other lipid levels, including total cholesterol (TC), high-density lipoprotein (HDL), and low-density lipoprotein (LDL) did not differ significantly across the four groups. Similarly, liver function markers, such as alanine aminotransferase (ALT) and aspartate aminotransferase (AST), were not significantly different between groups.

3.2. Serum lipid abnormalities unique to the transition from DM to DKD

To identify and differentiate the lipid levels in the serum of each group, we performed an untargeted lipidomic analysis. For lipid annotation, we matched the *m/z* values in the MS1 spectrum of the 419 features extracted using Progenesis QI with total ion normalization, and confirmed the presence of the characteristic product ions of different lipid classes in the function-2 spectrum acquired in MS^E mode by comparing with public and in-house databases. A total of 192 lipid species across 18 lipid classes, with a relative standard deviation of less than 30 % for relative abundance among quality control samples were annotated in the serum of patients from all groups (Fig. 2a). The differences in lipid profiles between the control, DM, and DKD groups were visualized using volcano plots (Fig. 2b), and the number of upregulated and downregulated lipids in each comparison is shown in Fig. 2c.

When comparing the DM and DKD groups to the control group, there was a shared pattern of lipid changes. Both groups exhibited a suppression in the levels of most phospholipid classes, including LPE, LPC, PE, PC, and PS. Certain sphingolipid classes, such as SM and lactosylceramide (LacCer), were also suppressed (Fig. 2b and c). This shared dysregulation suggests a common lipidomic shift in the progression of DM and its complications. Despite the common lipid changes between DM and DKD patients when compared to controls, the progression from DM to DKD was marked by distinct lipidomic differences. The lipid profiles of DKD patients showed a significant elevation in several lipid species when compared to DM patients. These included most of the previously mentioned phospholipid classes (LPE, PE, and PC), sphingolipid classes (Cer, and SM), and the neutral lipid DAG class. In contrast, several lipid species from LPC, and cholesterol esters (CE) classes were downregulated in DKD compared to DM (Fig. 2b and c). These findings suggest that while both DM and DKD patients share some lipidomic changes compared to control individuals, the transition from DM to DKD is characterized by a distinct elevation in specific lipid species. This distinct lipid profile in DKD patients may contribute to the progression of kidney dysfunction and could serve as a potential biomarker for early detection and disease monitoring in DKD.

Table 1
Baseline characteristics of study population stratified by groups.

Parameters	Ctrl	DM	DKD-E	DKD-A
No. of subjects	22	55	21	32
Male, n (%)	12 (54.5)	25 (45.5)	8 (38.1)	14 (43.8)
Age, years	59.0 ± 5.0	64.9 ± 8.9**	64.3 ± 9.5*	67.0 ± 13.8*
BMI, kg/m^2	23.7 ± 2.8	24.8 ± 3.9	25.8 ± 3.2*	24.4 ± 3.3
Laboratory data				
Serum HbA1c (%)	5.6 ± 0.4	7.5 ± 1.5***	7.0 ± 0.9***	7.6 ± 1.3***
eGFR, mL/min/1.73 m^2	95.4 ± 9.1	93.7 ± 16.4	93.9 ± 9.9	64.8 ± 31.1***/###/$$$
BUN, mmol/L	5.0 ± 1.4	5.5 ± 1.3	6.4 ± 2.5*/#	8.8 ± 4.4***/###/$
Serum creatinine, μmol/L	67.3 ± 11.6	64.0 ± 13.5	61.3 ± 13.0	123.5 ± 112.9*/###/$
Serum albumin, g/L	42.5 ± 2.4	42.8 ± 3.5	42.3 ± 2.5	39.5 ± 6.3*/##
UACR, mg/g	5.8 ± 2.9	9.6 ± 6.1**	103.0 ± 70.2***/###	937.8 ± 1048.0***/###/$$$
Serum uric acid, μmol/L	311.0 ± 85.8	334.0 ± 82.4	336.3 ± 79.6	376.4 ± 101.8*/#
Serum TG, mmol/L	1.4 ± 0.7	1.5 ± 0.9	1.9 ± 1.2	2.1 ± 1.4*/#
Serum TC, mmol/L	5.2 ± 0.9	4.9 ± 1.2	5.4 ± 1.5	5.1 ± 1.3
Serum HDL-C, mmol/L	1.6 ± 0.2	1.5 ± 0.3	1.6 ± 0.4	1.4 ± 0.3**/$
Serum LDL-C, mmol/L	3.5 ± 0.8	3.2 ± 0.9	3.6 ± 0.9	3.3 ± 1.1
ALT, U/L	21.5 ± 12.3	33.2 ± 33.4	32.1 ± 23.5	22.7 ± 12.6
AST, U/L	26.3 ± 7.6	26.9 ± 13.0	28.4 ± 14.5	24.0 ± 7.9

The values are expressed as means ± standard deviation (SD). HbA1c, glycosylated hemoglobin, type A1C; TG, triglycerides; eGFR, estimated glomerular filtration rate; BUN, blood urea nitrogen; UACR, urine albumin/creatinine ratio; TC, serum total cholesterol; HDL-C, high-density lipoprotein cholesterol; LDL-C, low-density lipoprotein cholesterol; ALT, alanine aminotransferase; AST, aspartate aminotransferase. Compared to Ctrl, *p < 0.05, **p < 0.01, and ***p < 0.001; compared to DM, #p < 0.05, ##p < 0.01, and ###p < 0.001; $p < 0.05, $$p < 0.01 and $$$p < 0.001 for DKD-E vs. DKD-A.

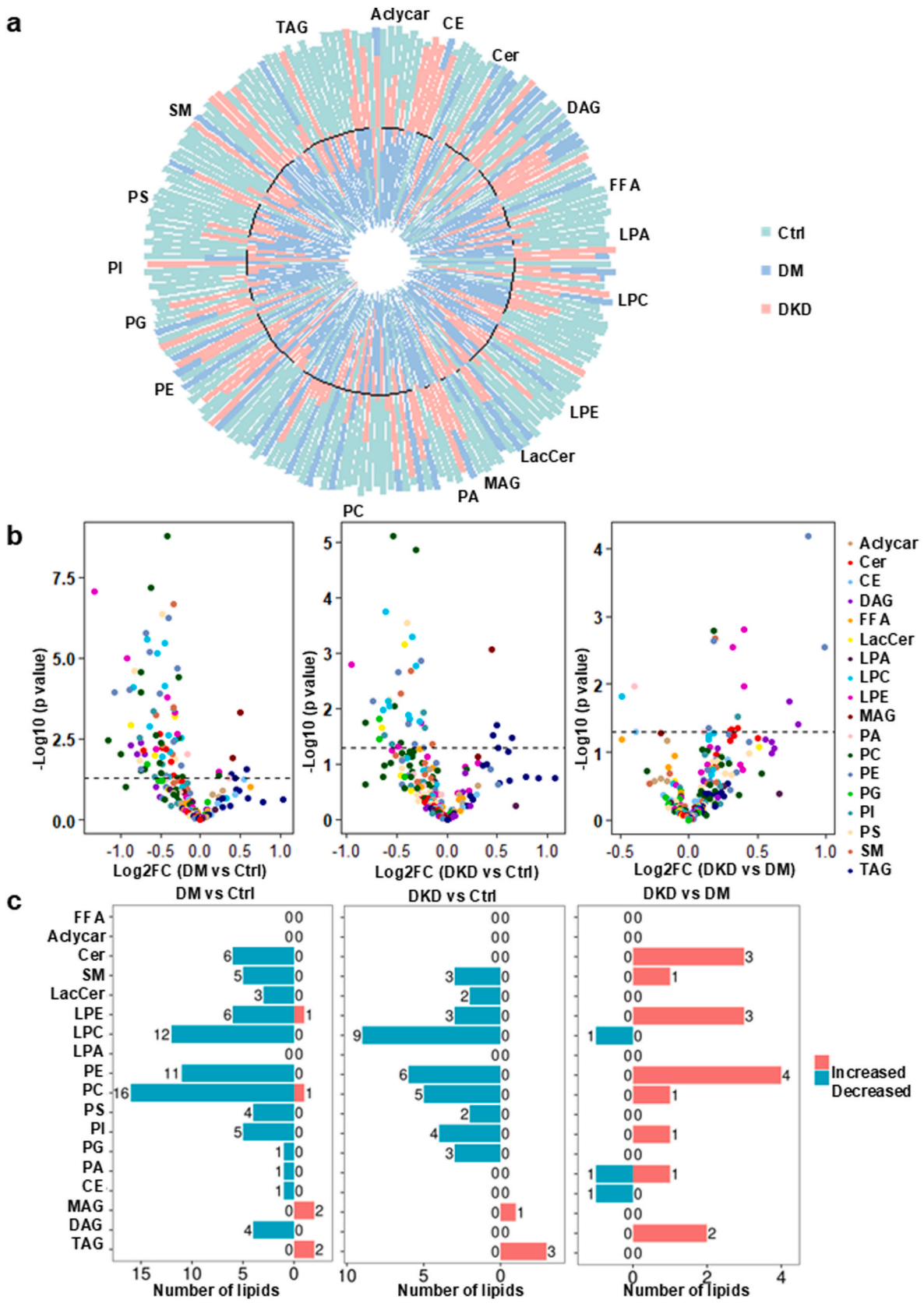

Fig. 2. Serum lipid abnormalities unique to the transition from DM to DKD. (a) Lipidome profiling among population with DM and DKD. **(b)** Volcano plots of the serum lipids of DM patients compared to Ctrl (left panel), DKD patients compared to Ctrl (middle panel), DKD patients compared to DM (right panel). **(c)** Specific amounts of differential lipids identified in B, with up-regulated lipids indicated in red and down-regulated lipids indicated in blue.

3.3. Different lipidomic shifts mark the DM to DKD progression

To further investigate the lipid alterations associated with the progression of DKD, we conducted a comparative analysis of the serum lipidome across the two distinct stages of DKD: the early stage (DKD-E) and the advanced stage (DKD-A). This exploration aimed to identify stage-specific lipid changes that may underlie the development of and progression of DKD. Partial least squares-discriminant analysis (PLS-DA) revealed that the lipidome profiles of the DM group were distinctly separated from the control group along principal component (PC1, $p = 0.052$) and PC2 ($p < 0.001$), from the DKD-E group in PC1 ($p < 0.05$), and from the DKD-A group in PC2 ($p < 0.001$). Additionally, the DKD-A group was clearly distinguished from DKD-E in PC2 ($p < 0.01$) (Fig. 3a and b). The heatmap results further confirmed that DKD-E and DKD-A had significantly different lipid distributions compared to the control and DM groups (Fig. 3c and Fig. S1). Unsupervised clustering of the detected lipids resulted in 5 major clusters. Among them, in Cluster 1, most lipids were both increased in DKD-E and DKD-A compared to DM, mainly including PCs, PEs, PSs and DAGs, as well as several lipids belonging to Cer, and phosphatidylinositol (PI) (Fig. 3c). Further investigation on the differential lipid between the DM group and the different stages of DKD revealed that compared to the DM group, significant upregulation of some lipid species from LPE, LPC, PE, PC, Cer, SM, monoacylglycerol (MAG), DAG, and TAG classes in DKD-E persisted into advanced stage, indicating the potential contribution of these lipids to the early onset and progression of DKD (Fig. 3d and e). Of note, in Cluster 2 as shown in Fig. 3c, most lipids remained similar between DM and DKD-E, but were elevated only in the DKD-A stage, including LPEs, LPCs and neutral lipids MAGs, and TAGs. Furthermore, compared to the DKD-E group, phospholipids, particularly several PCs, PEs, PSs and FFAs, were significantly decreased only in DKD-A group. In contrast, LPEs and LPCs exhibited a exclusive and remarkable elevation only in DKD-A group either compared to DM or DKD-E group, suggesting a potential role for the hydrolysis of phospholipids and the subsequent enrichment of lysophospholipids in the progression of DKD. Several TAG species were also increased in the DKD-A group compared to the early stage, consistent with clinical observations of more severe lipid accumulation in the kidneys of DKD-A patients [13]. In conclusion, our untargeted lipidomic analysis revealed distinct lipidomic shifts marking the transition from DM to DKD and progression through DKD stages. The upregulation of LPE, LPC, PE, PC, Cer, SM, MAG, DAG, and TAG classes probably contributes to the transition from DM to DKD, while the downregulation of PCs, PEs, and PSs, along with the upregulation of LPEs, LPCs, and TAGs is likely associated with the progression from DKD-E to DKD-A.

3.4. Specific lipid species patterns associated with DKD risk and severity

To identify serum lipids linked to DKD risk, we performed logistic regression analysis through univariate and multivariate analyses (Fig. 4a). The results demonstrated that age, gender, BMI and HbA1c didn't exhibited obvious correlation with the risk of DKD among DM population. Significant associations were observed between Cer, LPE, PE, and DAG classes with an increased risk of incident DKD. The odds ratios (OR) per standard deviation (SD) increment were as follows: LPE (OR: 2.81, 95 % CI 0.90–8.49, $p = 0.074$), LPC (OR: 2.80, 95 % CI 0.92–8.75, $p = 0.069$), PE (OR: 2.45, 95 % CI 0.93–6.47, $p = 0.070$), and DAG (OR: 1.77, 95 % CI 0.99–3.18, $p = 0.054$). Furthermore, among these lipid species, most LPE species, including LPE(16:0), LPE(18:0), LPE(18:1), LPE(22:0), LPE(22:1), LPE(22:2), two PE species, including PE(34:1) and PE(34:2), as well as three LPC species, including LPC (18:2), LPC(20:1), LPC(20:2), demonstrated a positive correlation with DKD severity markers such as UACR, SCr, and BUN, while showing an inverse association with eGFR and serum albumin (Fig. 4b). Most DAG species, including DAG(34:1), DAG(34:2), DAG(36:1), DAG(36:2), DAG (36:3), and DAG(36:4), also showed significantly positive associations with UACR, Scr, BUN and urinary creatinine, and inversely related with serum albumin. Collectively, most DAGs exhibited strong associations with UACR, Scr, BUN and urine microalbumin, the key indicators of DKD severity. Moreover, most LPEs, LPCs and some PEs simultaneously displayed significant positive correlations with UACR and inverse associations with eGFR, consistent with the positive effect of these lipids on the risk of DKD. These findings established the potential association between these key lipid species, particularly LPEs, LPCs, PEs, and DAGs with DKD risk and disease progression.

3.5. Alterations of LPE, PE, LPC, and DAG species in the progression from DM to DKD

To evaluate whether the lipid classes, LPE, PE, LPC, and DAG, exhibit a change pattern correlating with the progression of DKD, we analyzed the levels of specific lipid species within these five classes across four groups: Ctrl, DM, DKD-E, and DKD-A. As shown in Fig. 5, LPEs exhibited a declining trend in the DM group relative to Ctrl, followed by significant elevations noted only in the DKD-A group compared to both DM and DKD-E. This pattern was particularly evident for LPE species such as LPE (16:0), LPE(18:1), LPE(18:2), LPE(20:1), and LPE(20:2). The most abundant species in PEs, including PE(36:1), PE(36:2), and PE(38:2), and certain DAGs, such as DAG(34:1), DAG(34:2), DAG(36:2), and DAG (36:4), were significantly lower in the DM group compared to Ctrl. However, these lipids were conversely elevated in DKD groups when compared to DM, with no significant difference between DKD-E and DKD-A. Similarly, LPCs were significantly lower in the DM group relative to Ctrl, while the most abundant species in LPC, including LPC (16:0), LPC(18:0), and LPC(18:2), and other mino LPCs, such as LPC (20:3) and LPC(20:5), exhibited significant elevations noted only in the DKD-A group compared to DM. Taken together, the specific lipids from Cer, PE, LPE, and DAG classes showed an upward trend during the transition from DM to DKD, while most LPEs exhibited further elevation in the progression from DKD-E to DKD-A. These results suggest the potential involvement of PE, DAG, and LPC lipids in the development of DKD, while LPE likely plays a critical role in disease progression.

3.6. Performance Evaluation of a Lipid-Based Biomarker Panel for Early Identification of DKD from DM

Given the above-established risk-of-DKD associated lipids, we then propose a lipid-based biomarker panel to distinguish DKD from DM using three machine learning methods: random forest (RF), support vector machine-recursive feature elimination (SVM-RFE), and least absolute shrinkage and selection operator (LASSO) regression for variable screening. These methods were applied to identify the most significant lipid variables, which could serve as effective biomarkers for the early detection and progression of DKD.

By evaluating the top 15 variables identified by RF for distinguishing between DM and DKD (Fig. 6a), the 13 variables selected by SVM-RFE for maximum accuracy (Fig. 6b), and the 7 variables with non-zero coefficients in the Lasso regression model established with lambda.min (Fig. 6c), we selected nine lipid variables that appeared in at least two of the three sets, including LPC(18:2), LPC(20:5), LPE (16:0), LPE (18:0), LPE (18:1), LPE (24:0), PE (34:1), PE (34:2), and PE (36:2) (Fig. 6d). The abundance of these lipids, particularly LPE(16:0), LPE (18:0), PE(36:2), PE(34:1), and PE(34:2), showed a tendency to increase with rising UACR (Fig. 6e), indicating their potential enrichment during the transition from DM to DKD. To assess the predictive power of this nine-lipid panel (referred to as Lipid9 model), we compared it against two clinical indexes—SCr and BUN (abbreviated as SCB)—alone or in combination (Lipid9-SCB model), as well as against eGFR, in classifying patients with DKD from DM. Receiver operating characteristic (ROC) analysis revealed that that area under ROC curve (AUC) of Lipid9 was 0.78 (95 % CI 0.68–0.86), higher than that of SCB (AUC: 0.72, 95 % CI 0.62–0.82), and eGFR (AUC: 0.68, 95 % CI 0.58–0.78) (Fig. 6f). Thus,

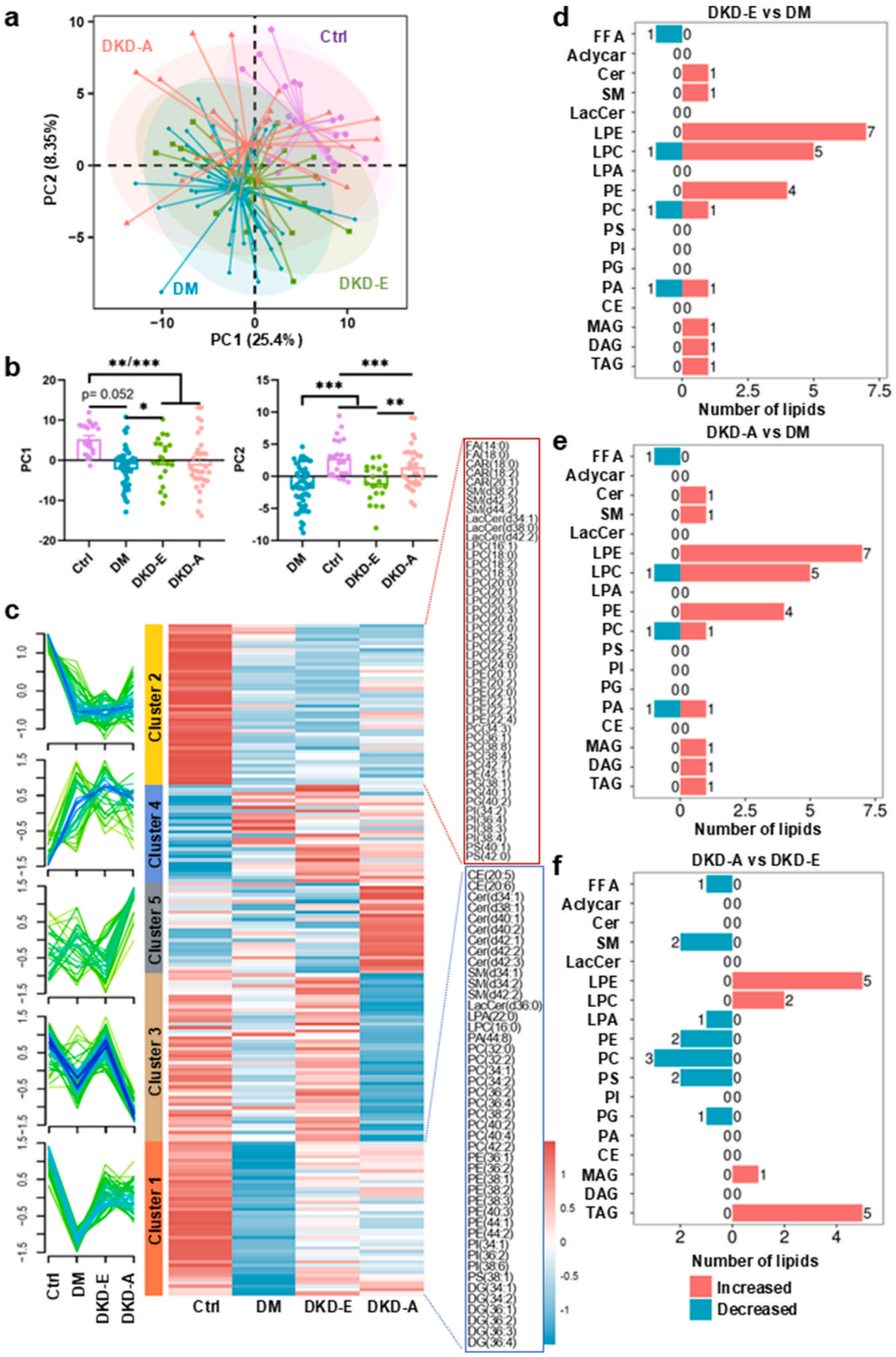

Fig. 3. Different lipidomic shifts Mark the DM to DKD progression. **(a)** PLS-DA plot of lipid species in Ctrl, DM, DKD-E, and DKD-A groups. **(b)** Comparison of principal component subject scores, PC1 (left panel) and PC2 (right panel) in the four groups. **(c)** Heatmap of all annotated lipids in serum lipids between the four groups clustered using mFuzz into significant discrete clusters. **(d–f)** Specific amounts of differential lipids of DKD-E compared to DM **(d)**, DKD-A compared to DM **(e)**, DKD-A compared to DKD-E **(f)**, with up-regulated lipids indicated in red and down-regulated lipids indicated in blue.

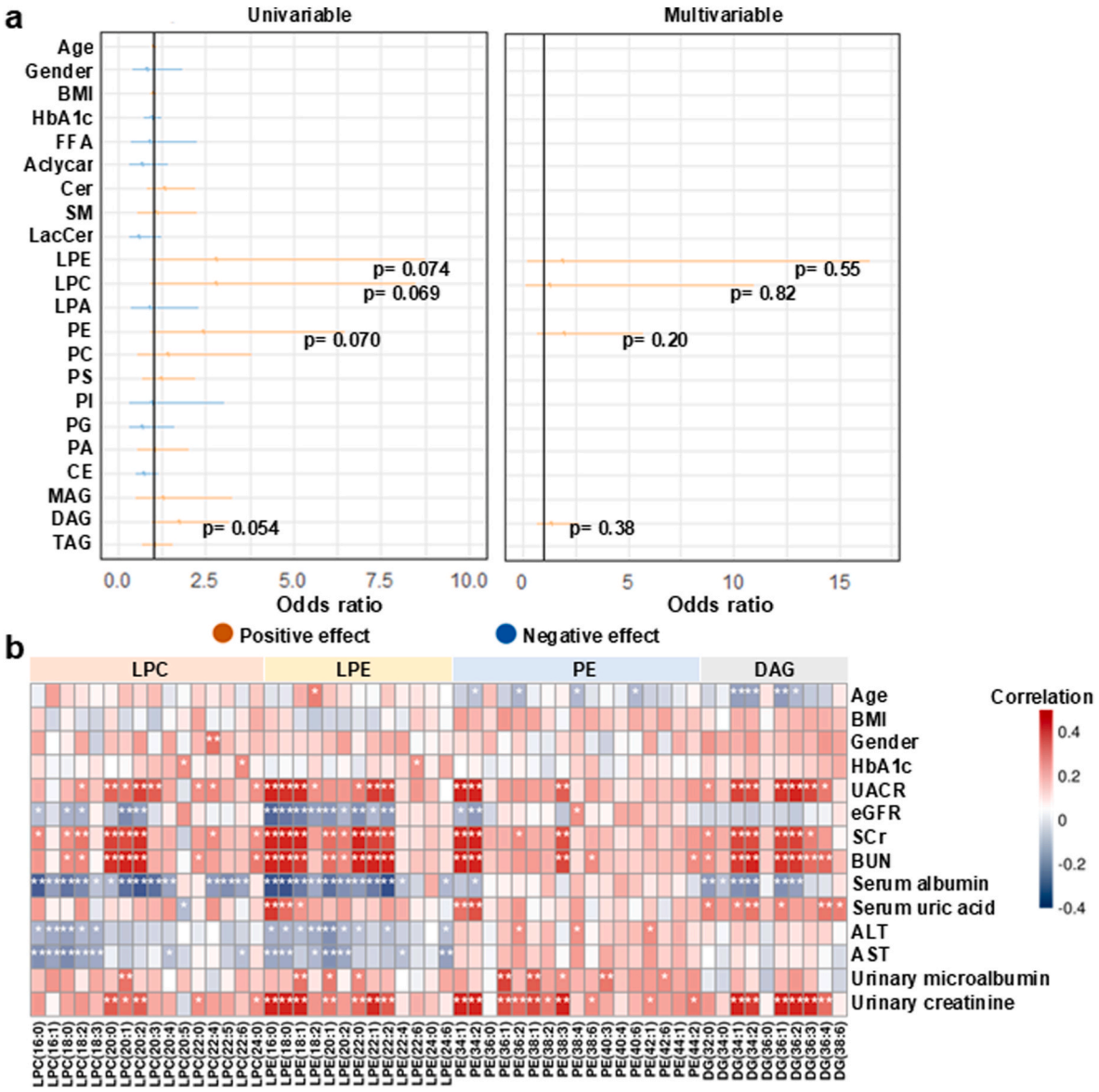

Fig. 4. Specific lipid species patterns associated with DKD Risk and severity. **(a)** Univariate (left panel) and multivariate (right) logistic regression for the evaluation of the association of each lipid class with the incident DKD in DM population. Forest plot of odds ratios (95 % CI) for DKD per lipid of specific changes in a DKD population with DM. Odds ratios are calculated for 1 SD of the explanatory variables. **(b)** Pearson's correlation analysis of the association of lipid species in LPC, LPE, PE, and DAG classes with clinical indicators. *p < 0.05, **p < 0.01, ***p < 0.001. The color key represents the regression coefficients of each variables.

the nine serum lipids were identified as potential DKD biomarkers. More importantly, the Lipid9-SCB combination yielded an even higher AUC of 0.82 (95 % CI 0.75–0.90), significantly surpassing the other models. The diagnostic performance of Lipid9-SCB showed higher sensitivity and specificity value of 0.84 and 0.75, respectively, at the optimal cutoff obtained based on Youden index when discriminating DKD from DM, than eGFR with sensitivity and specificity value of 0.61 and 0.61 at the cutoff of 90 mL/min/1.73 m^2 (CKD G2-G5) according to KDIGO guidelines. Furthermore, when identifying early DKD in DM patients, the Lipid9 model achieved an AUC of 0.75 (95 % CI 0.63–0.88), comparable to that of the Lipid9-SCB combination (AUC: 0.79, 95 % CI 0.67–0.91), both markedly better than SCB (AUC: 0.66, 95 % CI 0.52–0.80), and eGFR (AUC: 0.54, 95 % CI 0.39–0.68) (Fig. 6g). Similarly, the Lipid9 (AUC: 0.89 [0.83–0.96] and 0.84 [0.73–0.95], respectively) or Lipid9-SCB (AUC: 0.94 [0.88–0.99] and 0.92 [0.85–0.99], respectively) showed good performance in distinguishing advanced DKD from DM or DKD-E, outperforming SCB alone (AUC: 0.83 [0.73–0.93] and 0.85 [0.74–0.95], respectively) or eGFR (AUC: 0.82 [0.72–0.92] and 0.84 [0.74–0.94], respectively) (Fig. 6h and i).

In conclusion, the combination of the nine-lipid panel (Lipid9) with the clinical indexes SCr and BUN (Lipid9-SCB) shows great potential for early DKD detection and for differentiating its stages, with superior performance compared to existing clinical markers.

4. Discussion

The kidney is a highly energetically demanding organ that relies heavily on fatty acid oxidation for energy. Lipid homeostasis is considered to be crucial to maintain kidney function [27]. Dysregulation in lipid metabolism, such as aberration in FAO, lipid uptake and lipogenesis, promotes the progression of DKD. For example, in the kidney, the accumulation of excess fatty acids results in damage to podocytes, causing mitochondrial dysfunction, and injury to the glomeruli and tubulointerstitial tissue [28]. While traditional methods like eGFR and UACR remain cornerstone indicators, lipidomics provide complementary insights by capturing pathophysiological lipid remodeling linked to

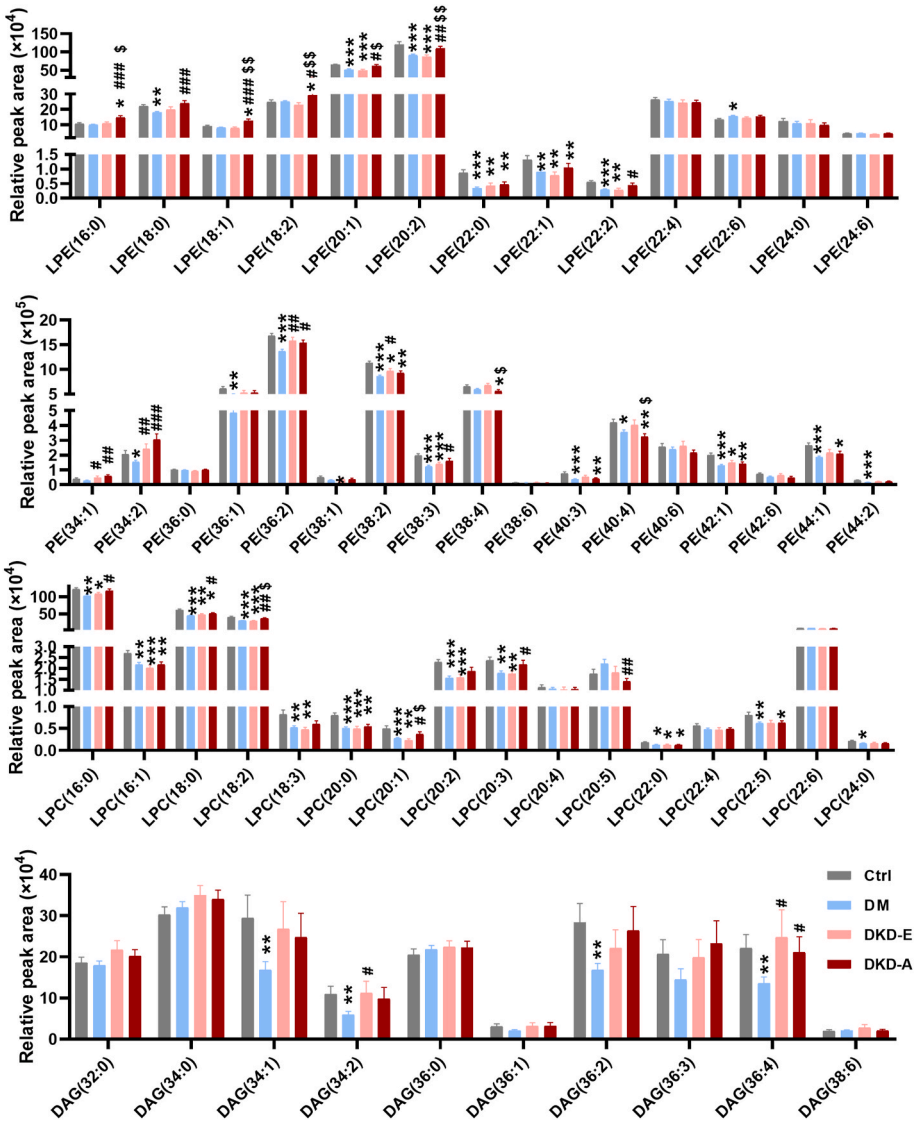

Fig. 5. Alterations of LPC, LPE, PE, and DAG Species in the Progression from DM to DKD. *p < 0.05, **p < 0.01, ***p < 0.001 compared to Ctrl. #p < 0.05, ##p < 0.01, ###p < 0.001 compared to DM. $p < 0.05, $$p < 0.01, $$$p < 0.001 compared to DKD-E.

tubular injury. Previous studies have suggested that lipotoxicity-associated renal damage is driven not only by the amount of lipids, but also by the specific lipid species accumulated in the kidney [27]. By identifying lipid species that are dysregulated in disease states, lipidomics can help in discovering potential therapeutic targets. Despite advancements in understanding dyslipidemia in DM and chronic kidney disease [13], the lipid signature associated with the transition from DM to DKD and progression of DKD remains unclear. In this study, we investigated the serum lipidomic changes associated with DKD onset and progression between DM, DKD-E and DKD-A patients, and identified systemic lipid markers of diagnostic value for early discrimination of DKD.

Regarding the lipid signature contributing to DKD progression, our study observed notably decreases in two phospholipid classes (PC and PS) and elevations in two lysophospholipid classes (LPE and LPC) in DKD-A group compared to DKD-E group. These findings suggest that hydrolysis of phospholipids and the subsequent accumulation of lysophospholipids may play a role DKD progression. Previous studies have linked increases in phospholipids [29] with DKD, aligning with our findings. In the CRIC cohort, intra-class mean of PEs were higher in the progressors as compared to the non-progressors [30]. Serum phospholipids including phosphatidylserine (PS), sphingomyelin (SM), and phosphatidylcholine (PC) were found to be significantly upregulated in the DKD group and were highly correlated with the ACR [31]. It is well-established that phospholipids are the predominant lipid class in the kidney, constituting more than 50 % of the total renal lipids. Among them, PE and LPE have been shown to be closely associated with DKD development. Afshinnia et al. examined serum samples from Amerindian populations with DKD and demonstrated that PE levels were significantly upregulated in DKD patients and were positively correlated with disease progression [32]. Additionally, PE aggregation was found in renal tubular cells from a DKD mouse model [33], further supporting its involvement. In their risk prediction model, a one-SD increase in PE was associated with a 1.78-fold increased risk of disease progression (95 % CI: 1.24–2.57, p = 0.002), confirming its potential as a biomarker for monitoring DKD progression [32]. In addition, the African American Study of Kidney Disease and Hypertension (AASK) and the Modification of Diet in Renal Disease (MDRD) studies identified six PEs significantly associated with proteinuria, a key marker of DKD progression [34]. Furthermore, Allison McCrimmon et al. identified four significantly oxidized PEs as the most oxidatively modified lipid subclass in the kidneys of *db/db* mice, suggesting that altered serum PE levels in DKD may be related to mitochondrial dysfunction [35]. However, a precise mechanistic link between PE and DKD progression has yet to be fully

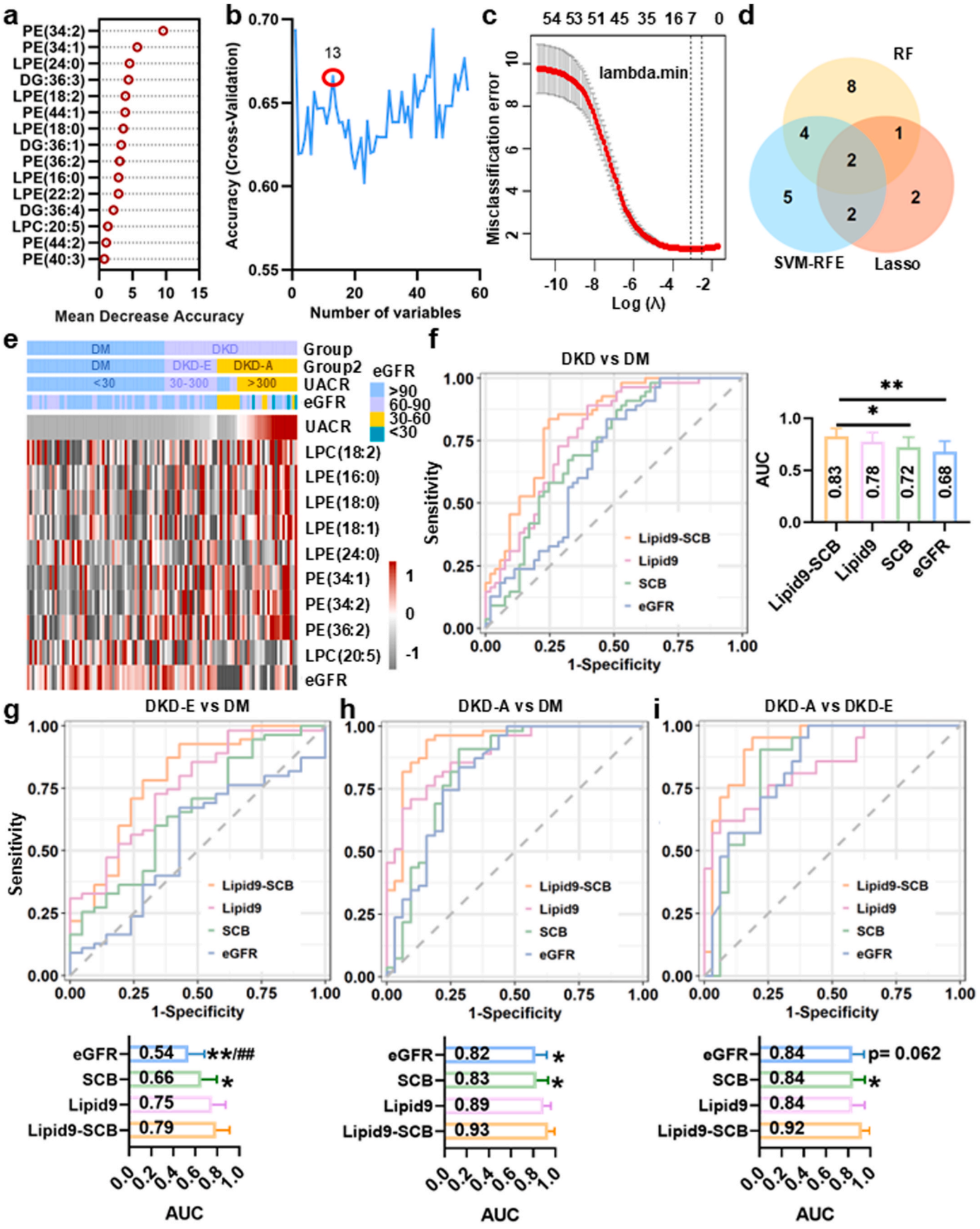

(caption on next page)

Fig. 6. Performance Evaluation of a Lipid-Based Biomarker Panel for Early Identification of DKD from DM. (a–c) Machine learning to identify the key lipids for the differentiating DKD from DM, including top 15 lipids ranked by RF **(a)**, 13 lipids selected by SVM-RFE**(b)**, and 7 lipids selected by LASSO regression method **(c)**. **(d)** Venn diagram illustrated that 9 lipids were identified by the three machine learning methods. **(e)** Heatmap displayed the levels of 9 lipids, as well as UACR and eGFR in DM and DKD populations. **(f)** Receiver operating characteristic curve (ROC) and AUC of 9 lipids alone (Lipid9) or in combination with 2 clinical indexes, including SCr and BUN (Lipid9-SCB), 2 clinical indexes (SCB), or eGFR alone to predict DKD among DM population. **(g–i)** ROC and AUC of Lipid9-SCB, Lipid9, SCB and eGFR for models to predict DKD-E **(g)** and DKD-A **(h)** among DM population and differentiating DKD-A from DKD-E **(i)**. *$p < 0.05$, **$p < 0.01$ compared to Lipid9-SCB. $^{\#\#}p < 0.01$ compared to Lipid9.

elucidated.

In the current study, LPE was significantly enriched in DKD-A, implying its potential involvement in DKD progression. LPE is a unique subclass of phospholipids, acting as membrane-derived bioactive lipid mediators. These molecules are derived from PE through partial catalysis by phospholipase A2 (PLA2) during glycerophospholipid metabolism [36]. Previous studies have also reported elevated levels of LPE in the kidneys of diabetic *db/db* mice [35], supporting the notion that LPE accumulation may be associated with DKD progression. LPEs are known to regulate various cellular processes, including inflammation, apoptosis, cytoskeletal rearrangement, and Ca^{2+} signaling. Thus, it may influence DKD pathophysiology by modulating inflammatory responses and cellular dynamics [37]. Dysregulation of LPE in hyperglycemic conditions, such as those seen in DKD, could impair cytoskeletal functions and cell motility, and promote disease progression [35]. Given the significant enrichment of LPE in advanced stages of DKD (DKD-A), this lipid subclass represents a promising target for further investigation.

We also observed changes in DAGs in DKD patients, suggesting their involvement in disease pathogenesis. DAG is a glyceride containing 2 fatty acyl groups, which is mainly involved in cell membrane formation [38] and synaptic vesicle cycling response [39], but also acts as a secondary lipid messenger, particularly in insulin signaling pathways [40]. A cohort study based on chronic renal insufficiency found that DAG in baseline samples was the most predictive lipid distinguishing progressors from non-progressors to ESKD [30]. The specific mechanism of elevated DAG may be related to aberrant activation of protein kinase C (PKC) [41,42], which has been implicated in promoting oxidative stress and inflammation, contributing to DKD progression.

This study has several strengths, including a well-defined clinical sample set and strict quality control in lipidomic analysis. However, there are limitations to this study. Although LPE, PE, LPC and DAG showed consistent correlations with a wide range of renal function markers, confirmation with other filtration markers such as cystatin C is yet to be achieved. Secondly, we need to externally validate the findings in independent cohorts. The predictive performance of the proposed biomarker panel may be influenced by unmeasured heterogeneity in genetic predisposition, inter-individual variability in dietary patterns, lifestyle factors (e.g., physical activity), and differential therapeutic interventions across the cohort. In addition, the impact of LPE, PE, LPC and DAG-mediated lipotoxicity on renal proximal tubule cells needs to be further explored.

In conclusion, our study expands the understanding of lipid signature changes and dysregulation in DKD, and identifies potential lipid markers for disease stratification. By emphasizing the importance of lipidomic profiling, our findings suggest that monitoring lipid levels could serve as a valuable tool for predicting DKD progression. Systematic lipid assessments may enable the early detection of individuals at risk for advancing DKD, thereby facilitating timely interventions to mitigate renal damage and improve patient outcomes.

CRediT authorship contribution statement

Xiaozhen Guo: Writing – review & editing, Writing – original draft, Formal analysis, Data curation, Conceptualization. **Zixuan Zhang:** Writing – original draft, Investigation, Formal analysis, Conceptualization. **Cuina Li:** Resources, Conceptualization. **Xueling Li:** Resources. **Yutang Cao:** Software, Methodology. **Yangyang Wang:** Software, Methodology. **Jiaqi Li:** Software, Methodology. **Yibin Wang:** Software, Methodology, Investigation. **Kanglong Wang:** Software, Methodology. **Yameng Liu:** Resources. **Cen Xie:** Writing – review & editing, Supervision, Conceptualization. **Yifei Zhong:** Supervision, Conceptualization.

Data availability

The raw lipidomics data have been deposited to Metabolomics Workbench and can be accessed directly via the dataset DOI: 10.21228/M8DV6H.

Funding

This study was supported by National Natural Science Foundation of China (82222071), and Shanghai Municipal Science and Technology Major Project, to C.X.; National Natural Science Foundation of China (82274451) and Shanghai Hospital Development center (SHDC2022CRD003), Demonstration Pilot Project for the Inheritance, Innovation, and Development of Traditional Chinese Medicine in Shanghai Pudong New Area (Construction of High-Level Research-Oriented Traditional Chinese Medicine Hospital, No. YC-2023-0901), Top Talent Project of the Oriental Talent Program, Famous Traditional Chinese Medicine Practitioner Studio Construction Project of Pudong New Area (No. PDZY-2025-0703) to Y.Z.; and National Natural Science Foundation of China (82104253) to X.G.

Conflict of interest

The authors declare that they have no conflicts of interest with the contents of this article.

Appendix A. Supplementary data

Supplementary data to this article can be found online at https://doi.org/10.1016/j.metop.2025.100354.

References

[1] Group IHS. Hypoglycaemia, cardiovascular disease, and mortality in diabetes: epidemiology, pathogenesis, and management. Lancet Diabetes Endocrinol 2019;7:385–96.
[2] Ogurtsova K, Guariguata L, Barengo NC, Ruiz PL, Sacre JW, Karuranga S, et al. IDF diabetes Atlas: global estimates of undiagnosed diabetes in adults for 2021. Diabetes Res Clin Pract 2022;183:109118.
[3] Association AD. 11. Microvascular complications and foot care: standards of medical care in diabetes-2021. Diabetes care. Diabetes Care 2021;44:S151–67.
[4] Selby NM, Taal MW. An updated overview of diabetic nephropathy: diagnosis, prognosis, treatment goals and latest guidelines. Diabetes Obes Metabol 2020;22 (Suppl 1):3–15.
[5] Livingstone SJ, Levin D, Looker HC, Lindsay RS, Wild SH, Joss N, et al. Estimated life expectancy in a Scottish cohort with type 1 diabetes, 2008-2010. JAMA 2015;313:37–44.
[6] Kato M, Natarajan R. Epigenetics and epigenomics in diabetic kidney disease and metabolic memory. Nat Rev Nephrol 2019;15:327–45.
[7] Macisaac RJ, Jerums G. Diabetic kidney disease with and without albuminuria. Curr Opin Nephrol Hypertens 2011;20:246–57.
[8] Kramer H, Boucher RE, Leehey D, Fried L, Wei G, Greene T, et al. Increasing mortality in adults with diabetes and low estimated glomerular filtration rate in the absence of albuminuria. Diabetes Care 2018;41:775–81.
[9] Zürbig P, Mischak H, Menne J, Haller H. CKD273 enables efficient prediction of diabetic nephropathy in nonalbuminuric patients. Diabetes Care 2019;42:e4–5.
[10] Abbasi F, Moosaie F, Khaloo P, Dehghani Firouzabadi F, Fatemi Abhari SM, Atainia B, et al. Neutrophil gelatinase-associated lipocalin and retinol-binding protein-4 as biomarkers for diabetic kidney disease. Kidney Blood Press Res 2020;45:222–32.

[11] Zuydam NRv, Ahlqvist E, Sandholm N, Deshmukh H, Rayner NW, Abdalla M, et al. A genome-wide association study of diabetic kidney disease in subjects with type 2 diabetes. Diabetes 2018;67:1414–27.
[12] DeBose-Boyd RA. Significance and regulation of lipid metabolism. Semin Cell Dev Biol 2018;81:97.
[13] Lee LE, Doke T, Mukhi D, Susztak K. The key role of altered tubule cell lipid metabolism in kidney disease development. Kidney Int 2024;106:24–34.
[14] Ma H, Guo X, Cui S, Wu Y, Zhang Y, Shen X, et al. Dephosphorylation of AMP-activated protein kinase exacerbates ischemia/reperfusion-induced acute kidney injury via mitochondrial dysfunction. Kidney Int 2022;101:315–30.
[15] Alla Mitrofanova GB, Merscher Sandra, Fornoni Alessia. New insights into renal lipid dysmetabolism in diabetic kidney disease. World J Diabetes 2021;12:524–40.
[16] Tofte N, Suvitaival T, Ahonen L, Winther SA, Theilade S, Frimodt-Møller M, et al. Lipidomic analysis reveals sphingomyelin and phosphatidylcholine species associated with renal impairment and all-cause mortality in type 1 diabetes. Sci Rep 2019;9:16398.
[17] Xu T, Xu X, Zhang L, Zhang K, Wei Q, Zhu L, et al. Lipidomics reveals serum specific lipid alterations in diabetic nephropathy. Front Endocrinol 2021;12:781417.
[18] Wen CP, Chang CH, Tsai MK, Lee JH, Lu PJ, Tsai SP, et al. Diabetes with early kidney involvement may shorten life expectancy by 16 years. Kidney Int 2017;92:388–96.
[19] Stevens PE, Ahmed SB, Carrero JJ, Foster B, Francis A, Hall RK, et al. KDIGO 2024 clinical practice guideline for the evaluation and management of chronic kidney disease. Kidney Int 2024;105:S117–314.
[20] Fan Y, Yi Z, D'Agati VD, Sun Z, Zhong F, Zhang W, et al. Comparison of kidney transcriptomic profiles of early and advanced diabetic nephropathy reveals potential new mechanisms for disease progression. Diabetes 2019;68:2301–14.
[21] Inker LA, Eneanya ND, Coresh J, Tighiouart H, Wang D, Sang Y, et al. New creatinine- and cystatin C-based equations to estimate GFR without race. N Engl J Med 2021;385:1737–49.
[22] Levey AS, Stevens LA, Schmid CH, Zhang YL, Castro 3rd AF, Feldman HI, et al. A new equation to estimate glomerular filtration rate. Ann Intern Med 2009;150:604–12.
[23] Bzdok D, Altman N, Krzywinski M. Statistics versus machine learning. Nat Methods 2018;15:233–4.
[24] Friedman J, Hastie T, Tibshirani R. Regularization paths for generalized linear models via coordinate descent. J Stat Software 2010;33:1–22.
[25] Noble WS. What is a support vector machine? Nat Biotechnol 2006;24:1565–7.
[26] Hu J, Szymczak S. A review on longitudinal data analysis with random forest. Briefings Bioinf 2023;24.
[27] Baek J, He C, Afshinnia F, Michailidis G, Pennathur S. Lipidomic approaches to dissect dysregulated lipid metabolism in kidney disease. Nat Rev Nephrol 2021;18:38–55.
[28] Zhang H, Zuo J-j, Dong S-s, Lan Y, Wu C-w, Mao G-y, et al. Identification of potential serum metabolic biomarkers of diabetic kidney disease: a widely targeted metabolomics study. J Diabetes Res 2020;2020:1–11.
[29] Yoshioka K, Hirakawa Y, Kurano M, Ube Y, Ono Y, Kojima K, et al. Lysophosphatidylcholine mediates fast decline in kidney function in diabetic kidney disease. Kidney Int 2022;101:510–26.
[30] Afshinnia F, Rajendiran TM, Karnovsky A, Soni T, Wang X, Xie D, et al. Lipidomic signature of progression of chronic kidney disease in the chronic renal insufficiency cohort. Kidney Int Rep 2016;1:256–68.
[31] Ye S, Hu Y-p, Zhou Q, Zhang H, Xia Z-z, Zhao S-z, et al. Lipidomics profiling reveals serum phospholipids associated with albuminuria in early type 2 diabetic kidney disease. ACS Omega 2023;8:36543–52.
[32] Afshinnia F, Nair V, Lin J, Rajendiran TM, Soni T, Byun J, et al. Increased lipogenesis and impaired β-oxidation predict type 2 diabetic kidney disease progression in American Indians. JCI Insight 2019;4.
[33] Sas KM, Lin J, Rajendiran TM, Soni T, Nair V, Hinder LM, et al. Shared and distinct lipid-lipid interactions in plasma and affected tissues in a diabetic mouse model. J Lipid Res 2018;59:173–83.
[34] Luo S, Coresh J, Tin A, Rebholz CM, Appel LJ, Chen J, et al. Serum metabolomic alterations associated with proteinuria in CKD. Clin J Am Soc Nephrol : CJASN 2019;14:342–53.
[35] McCrimmon A, Corbin S, Shrestha B, Roman G, Dhungana S, Stadler K. Redox phospholipidomics analysis reveals specific oxidized phospholipids and regions in the diabetic mouse kidney. Redox Biol 2022;58:102520.
[36] Yamamoto Y, Sakurai T, Chen Z, Inoue N, Chiba H, Hui SP. Lysophosphatidylethanolamine affects lipid accumulation and metabolism in a human liver-derived cell line. Nutrients 2022;14.
[37] Meyer zu Heringdorf D, Jakobs KH. Lysophospholipid receptors: signalling, pharmacology and regulation by lysophospholipid metabolism. Biochim Biophys Acta 2007;1768:923–40.
[38] Janssen CI, Kiliaan AJ. Long-chain polyunsaturated fatty acids (LCPUFA) from genesis to senescence: the influence of LCPUFA on neural development, aging, and neurodegeneration. Prog Lipid Res 2014;53:1–17.
[39] Tu-Sekine B, Goldschmidt H, Raben DM. Diacylglycerol, phosphatidic acid, and their metabolic enzymes in synaptic vesicle recycling. Adv Biol Regulat 2015;57:147–52.
[40] Almena M, Mérida I. Shaping up the membrane: diacylglycerol coordinates spatial orientation of signaling. Trends Biochem Sci 2011;36:593–603.
[41] Kawanami D, Matoba K, Utsunomiya K. Signaling pathways in diabetic nephropathy. Histol Histopathol 2016;31:1059–67.
[42] Wang QJ. PKD at the crossroads of DAG and PKC signaling. Trends Pharmacol Sci 2006;27:317–23.